

Size Controlled Synthesis and Magnetic Properties of Ni-Zn Ferrite Nanoparticles by using Aloe Vera Extract Solution

SANJAY KUMAR¹, ASHWANI SHARMA¹, M. SINGH², POOJA DHIMAN²
and R.K. KOTNALA³

¹Department of Physics,
M. D. University, Rohtak- 124001, India

²Department of Physics,
H. P. University, Shimla- 171005, India

³Multiferroics and Magnetic Standards,
National Physical Laboratory, New Delhi-110012, India

ABSTRACT

$\text{Ni}_x \text{Zn}_{1-x} \text{Fe}_2 \text{O}_4$ ($x = 2.5, 4.5, 6.5, 8.5$) ferrite nanoparticles were prepared by a modified sol-gel method using high purity metal nitrates and aloe vera plant extracted solution. Using of aloe vera extract simplifies the process, provide an alternative process for a simple and economical synthesis of nanocrystalline ferrite and controlled size of $\text{Ni}_x \text{Zn}_{1-x} \text{Fe}_2 \text{O}_4$ ferrite nanoparticles were prepared. The structural characteristics of calcined sample of $\text{Ni}_x \text{Zn}_{1-x} \text{Fe}_2 \text{O}_4$ ($x = 2.5, 4.5, 6.5, 8.5$) ferrite nanoparticles were determined by X-ray diffraction (XRD), Fourier transform infrared spectroscopy (FTIR) and Transmission Electron Microscopy (TEM). All the prepared samples have spinel structure with particle size from 9 nm-20 nm. From XRD we observed that particle size decreases with increasing Ni content. Nano size of the particles was confirmed by TEM measurement. Magnetization measurements were obtained at room temperature by using Vibrating sample magnetometer (VSM), which showed that the calcined samples exhibited typical magnetic behaviour.

Keywords: Sol-gel, Aloe-vera, Synthesis, Magnetic properties, Electron microscopy, Spinel.

INTRODUCTION

Ni-Zn ferrites are soft magnetic material is mostly used as various

inductance components, such as magnetic cores of filters, transformers, deflection, antenna, video magnetic heads and magnetic heads of multiple path communication and

so on. Furthermore, the material has also brought potential applications in magnetic liquid absorbing materials (1-7). With rapid development of electronic information industries such as communications and computer networks, the size of electronic apparatus and equipments is miniaturized (8-9). Demand for electronic components with high density, light weight, thin type and fine performance is greatly increasing, which accelerate the demand for soft magnetic ferrites with high performance and thus contributes to the development of soft magnetic ferrites on the direction of higher frequency and lower power consumption (10-15). Ferrite particles in nano scales can be produced by soft chemical methods, such as co-precipitation, sol-gel and hydrothermal synthesis (16-17). Among other established synthesis methods, simple and cost effective routes to synthesize nanocrystalline Ni-Zn Fe_2O_4 by utilization of cheap, non-toxic and environmentally benign precursors are still the key issue.

Recently, biosynthesis is an alternative synthesis method to prepare nanocrystalline inorganic materials. There are many reports on the metal and semiconductor nanoparticles using fungi, actinomycetes and plant extracts. Aloe vera is (*Aloe barbadensis* Miller) is a perennial succulent belonging to the Liliaceal family. It is a cactus-like plant that grows in hot, dry climates. Aloe is a plant that grows in several parts of India and in several other countries. There is 99.5% water content in the aloe vera leaves and the rest is solid materials containing over 75 different ingredients including vitamins, minerals, enzymes, sugars, anthraquinones or phenolic compounds, lignin, saponins, sterols, amino

acids and salicylic acid. Aloe vera is gel is widely used in cosmetics industry as a hydrating ingredient in liquids, creams, sun lotions, lip balms, healing ointments etc. The gel is further used in pharmacology for wound healing, anti-inflammatory and burn treatment.

Chandran *et al.*¹⁸ have demonstrated the synthesis of nanotriangle gold and nanosilver using aloe vera plant extracts as a reducing agent. In this work, the sizes of nano triangle gold were about 50-350 nm and nano silver were about 5-15 nm (19). In this present work, we report for the first time the synthesis of nano particles of $\text{NiZnFe}_2\text{O}_4$ ferrite with crystallite size of 17.8 - 31.7 nm by simple modified Sol Gel method using metal nitrates and aloe vera extract solution as a precursors. The samples were characterized by XRD, FTIR and TEM. The magnetic properties of prepared nanoparticles were investigated by vibrating sample magnetometer (VSM).

2. EXPERIMENTAL DETAILS

All materials were of analytical grade and were used without further purification. Distilled water was used in all experiments.

In this study, the $\text{Ni}_x \text{Zn}_{1-x} \text{Fe}_2 \text{O}_4$ ferrite nanoparticles were synthesized by the modified sol-gel method. In this study either $\text{Zn}(\text{NO}_3)_2 \cdot 6\text{H}_2\text{O}$ or $\text{Ni}(\text{NO}_3)_2 \cdot 6\text{H}_2\text{O}$ mixed with $\text{Fe}(\text{NO}_3)_3 \cdot 9\text{H}_2\text{O}$ were used as the starting materials. In a typical procedure, 60 ml of aloe vera plant extract, instead of toxic organic polymers, was mixed with 40 ml distilled water under vigorous stir until homogeneous solution was obtained. According to this formula $\text{Ni}_x \text{Zn}_{1-x} \text{Fe}_2 \text{O}_4$

($x = 2.5, 4.5, 6.5, 8.5$), each metal nitrate was added slowly to the aloe vera solution under vigorous stirring for 2 h to obtain a well dissolved solution. No pH adjustment was made. Then the mixed solution was evaporated by heating on the hot plate at 100 °C under vigorous stirring for several hours until a dried precursor was obtained. The dried precursor was crushed into powder using mortar and pestle. The dried precursor then was calcined in a muffle – furnace at 600 °C for 2 h.

The X- ray diffraction (XRD) patterns of the samples were recorded on a PANalytical X'Pert PRO X-ray diffractometer using Cu K α radiation ($\lambda = 0.15406$ nm). The crystallite size of nanocrystalline samples was measured from the line broadening analyses using Debey-Scherrer formula after accounting for instrumental broadening.

$$D_{\text{XRD}} = 0.89 \lambda / \beta \cos \theta \quad (1)$$

Where λ – wavelength of X-ray radiation used in Å, θ is the diffraction angle, β is the full width at half maximum (FWHM) in radians in the 2θ scale, D_{XRD} is the crystallite size in nm.

The particle morphology was examined by Transmission Electron Microscopy (HITACHI). For the TEM observations, powders were supported on carbon-coated copper grids which was ultrasonically dispersed in ethanol.

Room temperature magnetic measurements were carried out using a Lakeshore vibrating sample magnetometer (VSM) and parameters like specific saturation magnetization (Ms), coercive force (Hc) and remanence (Mr) were evaluated.

FTIR spectra were recorded for dried samples of $\text{Ni}_x \text{Zn}_{1-x} \text{Fe}_2 \text{O}_4$ ($x = 2.5, 4.5, 6.5, 8.5$) with a varying from 0 to 1.0 with an Perkin – Elmer FTIR spectrometer. The dried samples were in KBR matrix, and spectra were measured according to transmittance method.

3. RESULT AND DISCUSSION

3.1. XRD Analysis

Generally, XRD can be used to characterize the crystallinity of nanoparticles. And it gives the average diameters of all the nanoparticles. The fine particles were characterized by XRD for structural determination and for estimation of crystallite size, XRD pattern were analyzed. All experimental peaks were matched with theoretically generated one and are indexed. The XRD patterns of all the samples were shown in Fig.1. It shows the formation of spinel ferrite phase in all the samples. The broad XRD line indicates that the ferrite particles are in nano size. The crystallite size for each composition are calculated from XRD line width of the (311) peak using Scherrer formula (20). The average crystallite size decreases from 20.0 nm to 9.0 nm when the partial substitution of Ni increases ($x = 2.5$ to $x = 8.5$). Though all samples were prepared under identical condition. The crystallite size was not the same for all the Ni concentrations. This was probably due to the preparation condition followed here which gave rise to different rate of ferrite formation for different concentrations of Nickel, favoring the variation of crystallite size. The values of the particle size, lattice constant as deduced from X-ray data are given by Table 1. The

lattice constant was found to decrease from 8.359 Å to 8.321 Å with increase in Ni concentration.

The strongest reflection comes from the (311) plane. Which denotes the spinel phase. All the compositions had a spinel structure. The peaks indexed to (200), (311), (400), (422), (511) and (440) planes of a cubic unit cell, corresponds to cubic spinel structure. The calculated lattice constant (Å), identified the sample to be cubic spinel.

3.2 Transmission Electron Microscopy

The morphology and structure of the prepared ferrite samples calcinated at 600 °C were investigated by TEM techniques as shown in figure 2. The results indicate that the samples prepared by sol-gel method are almost uniform in both morphology and particle size distribution. A close inspection would reveal the presence of particles showing the spherical in shape. The particle sizes increased with increasing Nickel concentration. The highest particle size obtained in this study was 20 nm at ($x = 2.5$) and particle size reached 9 nm at ($x = 8.5$). Mean particle size from TEM image is in good agreement with the crystallite size measured from X-ray line (311) broadening using Scherrer's formula. It may be mentioned here that in normal temperature and other methods it is not possible to control the particle size with improved magnetic properties. This is lower than the particle size of nanoferrites prepared by other chemical method.

3.3 Fourier Transform Infrared Analysis (FTIR) measurements

In order to confirm the formation of the spinel phase and to understand the nature

of the residual carbon in the samples, The FTIR spectra of the $\text{Ni}_x\text{Zn}_{1-x}\text{Fe}_2\text{O}_4$ ($x = 2.5, 4.5, 6.5, 8.5$) nanopowder calcined at 600 °C were recorded. The results from FTIR technique are presented in Fig.3. The calcined samples show characteristic absorptions of ferrite phase with a strong absorption around 600 cm^{-1} and weak absorption around 430 cm^{-1} . Murthy et al (21) have studied the IR absorption in Ni-Zn ferrite. This difference in the spectral positions is expected because of the difference in the $\text{Fe}^{3+}\text{-O}^{2-}$ distance for the octahedral and tetrahedral compounds (22). Waldron (23) studied the vibrational spectra of ferrites and attributed the sharp absorption band around 600 cm^{-1} to the intrinsic vibrations of the tetrahedral groups which corresponding restoring force causes stretching of $\text{Fe}^{3+}\text{-O}^{2-}$ bonds and the other band around 430 cm^{-1} is attributed to vibration of octahedral groups which are the bond bending vibrations. There are two weak and broad absorption peaks at around 1400 and 1600 cm^{-1} corresponding to the presence of small amounts of residual carbon in the samples. These absorptions in the present case are very weak which indicates that the residual carbon has mostly burnt away during the calcination process.

3.4 Magnetic Measurements

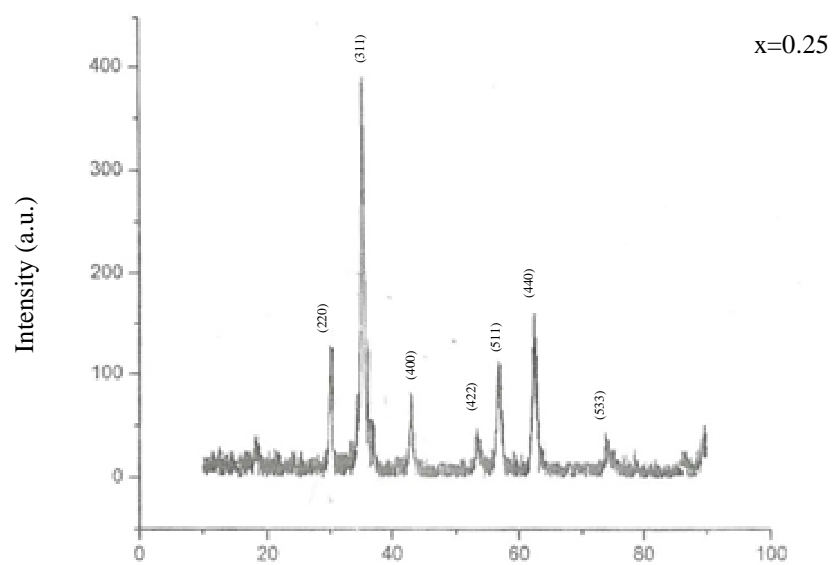
It is known that the magnetic parameters, particularly magnetizations and coercivity, of nano ferrites prepared by sol-gel method are different from those prepared by ceramic methods. The magnetic hysteretic loops of $\text{Ni}_x\text{Zn}_{1-x}\text{Fe}_2\text{O}_4$ Ferrite nanoparticles are given in Fig. 4. Variation of saturation magnetization with composition of series has been studied.

Among studied ferrites $\text{Ni}_{0.65}\text{Zn}_{0.35}\text{Fe}_2\text{O}_4$ has the highest specific magnetization. Note this composition contains middle level of Ni and Zn. This is because the different composition result in different particle sizes of ferrite samples as shown in table 1. It is known that magnetization in ferrites proceeds through the movement of the domain walls and domain rotations and the coercive force is obtained by reversal of the directions of the

wall movement and that of the domain rotation. The larger the particle size, the greater the probability of domain formation and domain rotation (24-26). On other hand, the smaller the particles contain less domain walls and require higher force for demagnetization (27). For smaller particles $\text{Ni}_{0.85}\text{Zn}_{0.15}\text{Fe}_2\text{O}_4$, the probability of domain rotation is higher and consequently the coercive force obtained is higher.

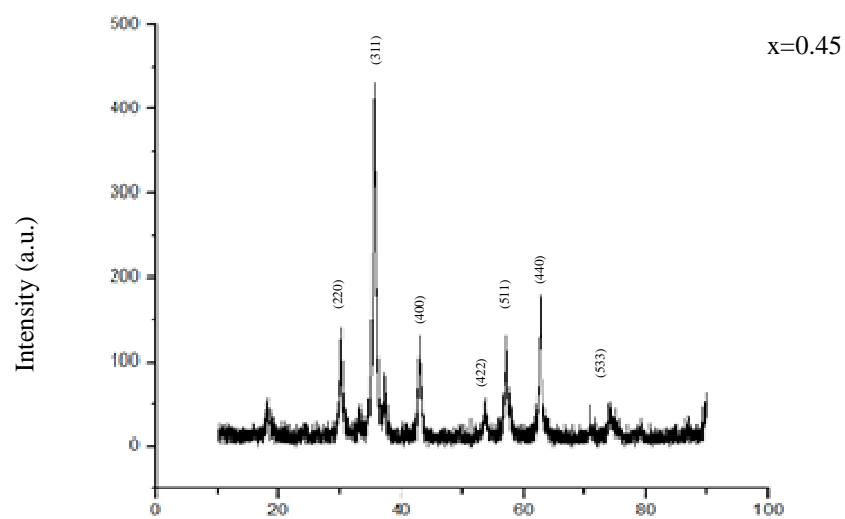
Table 1. Average particle size (nm) of $\text{Ni}_x\text{Zn}_{1-x}\text{Fe}_2\text{O}_4$ (x = 2.5, 4.5, 6.5, 8.5) ferrite nanoparticles determined from XRD , lattice constant and magnetization (emu/g) of $\text{Ni}_x\text{Zn}_{1-x}\text{Fe}_2\text{O}_4$ (x = 2.5, 4.5, 6.5, 8.5) ferrite nanoparticles calcined at 600°C for 2h

Composition	Particle size(nm)	Lattice constant (°A)	Magnetization (emu/g)
X = 2.5	20.0	8.359	00.84
X = 4.5	16.1	8.335	00.95
X = 6.5	15.6	8.323	11.71
X=8.5	09.0	8.321	03.54



(a)

2 Theta (Degree)



(b)

2 Theta (Degree)

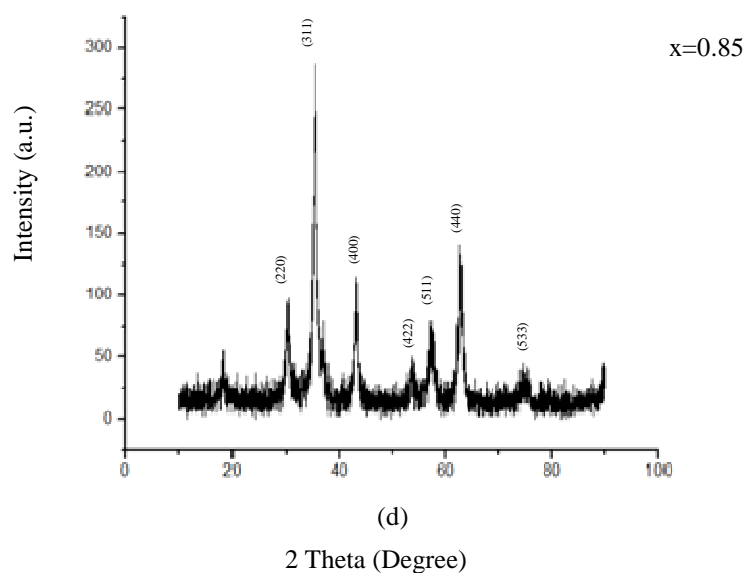
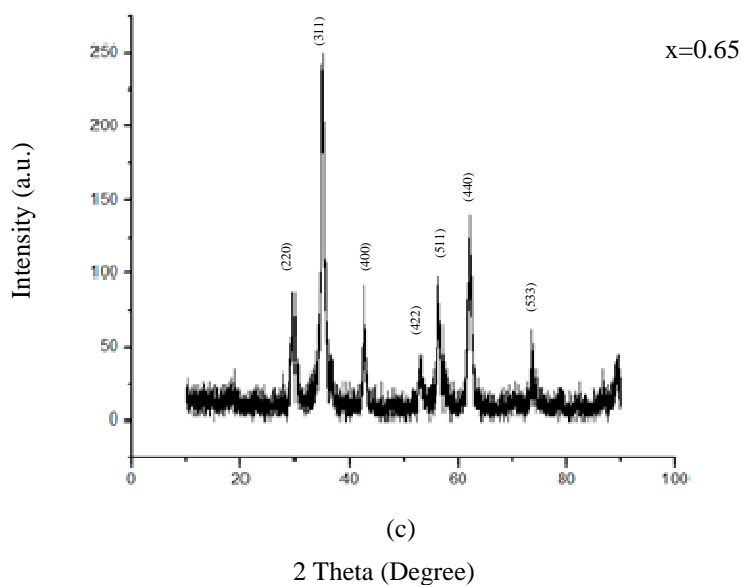


Figure 1: XRD patterns of $\text{Ni}_x\text{Zn}_{1-x}\text{Fe}_2\text{O}_4$ ferrites nanoparticles with $x=0.25, 0.45, 0.65, 0.85$ calcined at 600°C for 2h

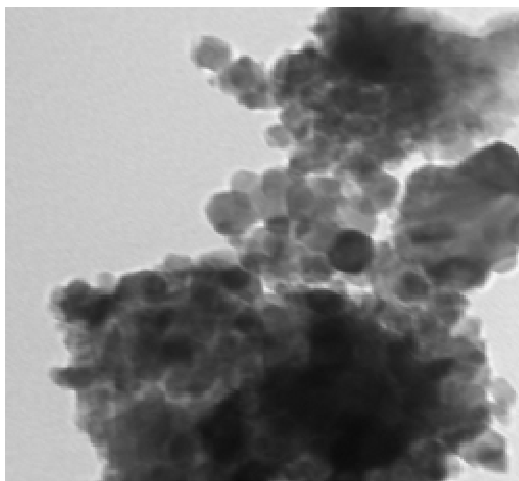
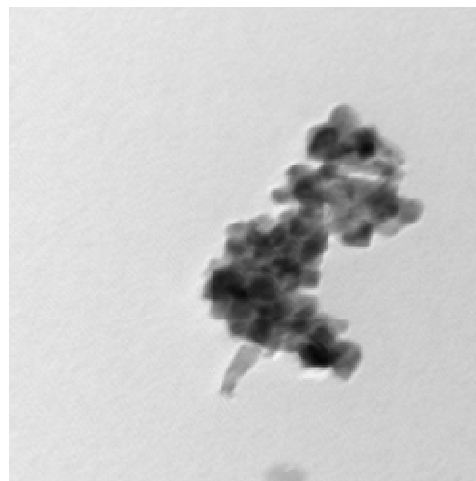
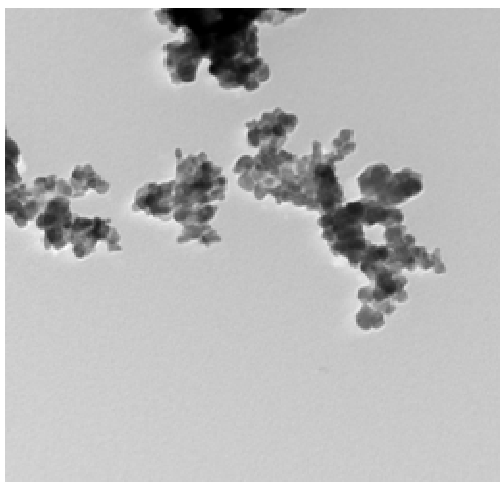
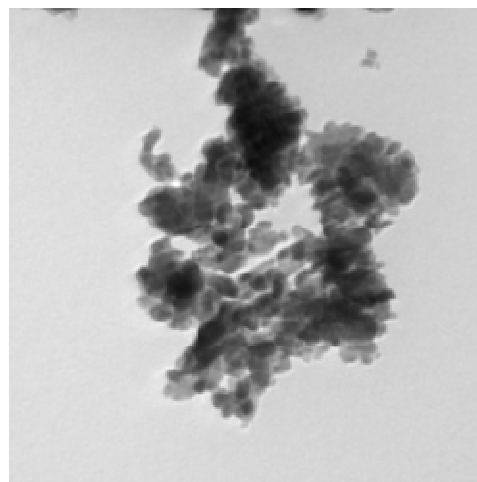
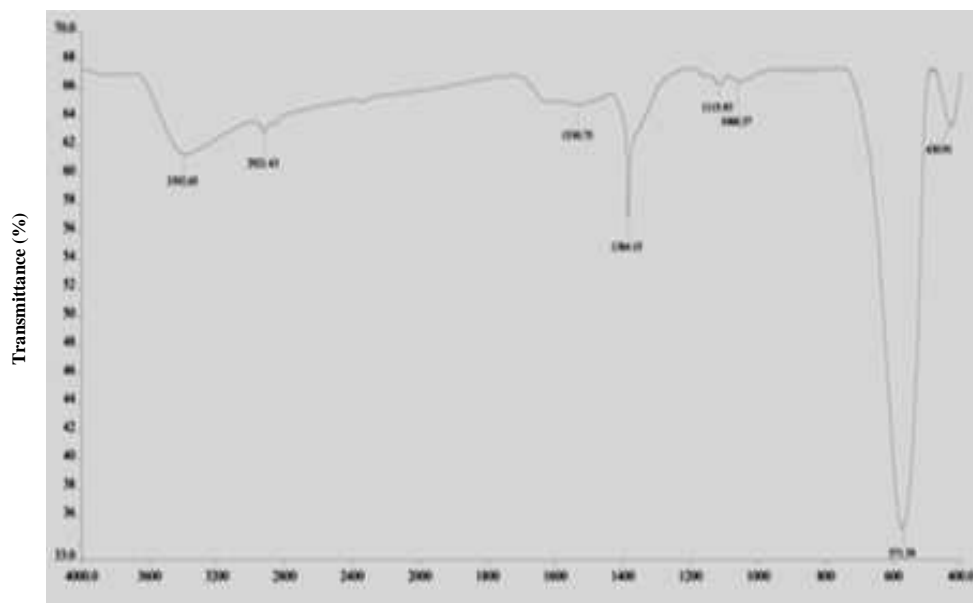
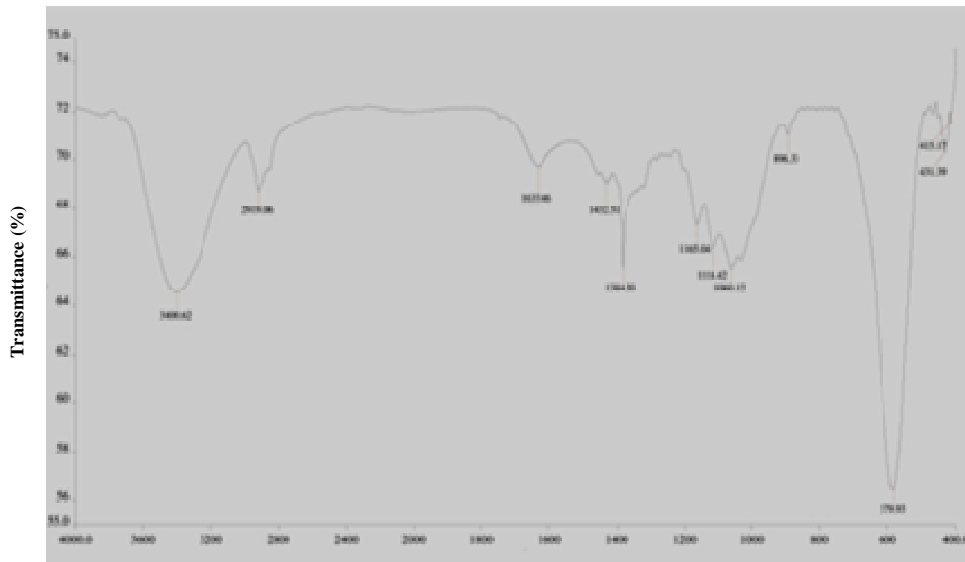
(a) $x = 0.25$ (b) $x = 0.45$ (c) $x = 0.65$ (d) $x = 0.85$

Figure 2: TEM images of $\text{Ni}_x\text{Zn}_{1-x}\text{Fe}_2\text{O}_4$ ferrites nanoparticles with $x=0.25, 0.45, 0.65, 0.85$ calcined at 600°C for 2h

(a) $x = 0.25$ Wave number (cm^{-1})(b) $x = 0.45$ Wave number (cm^{-1})

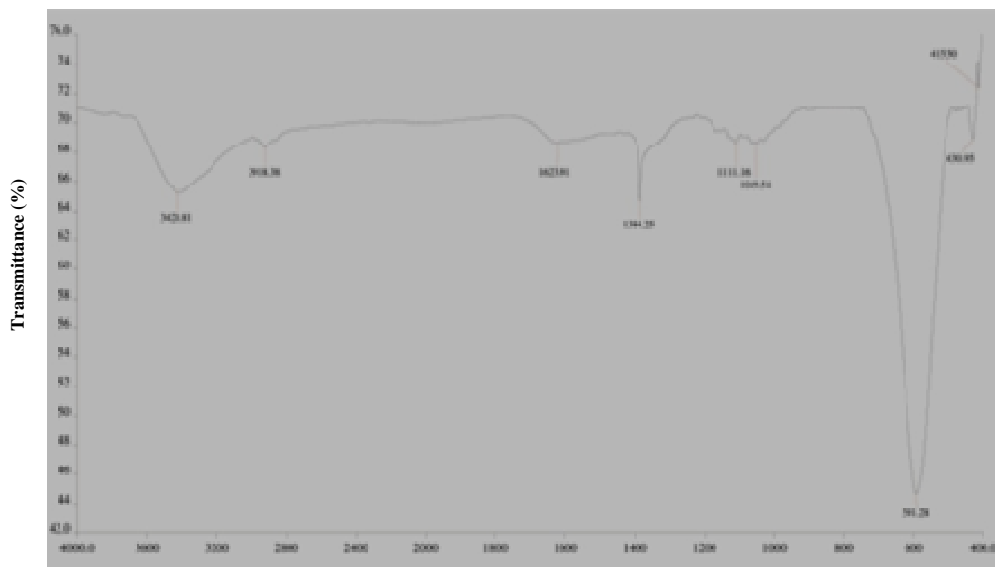
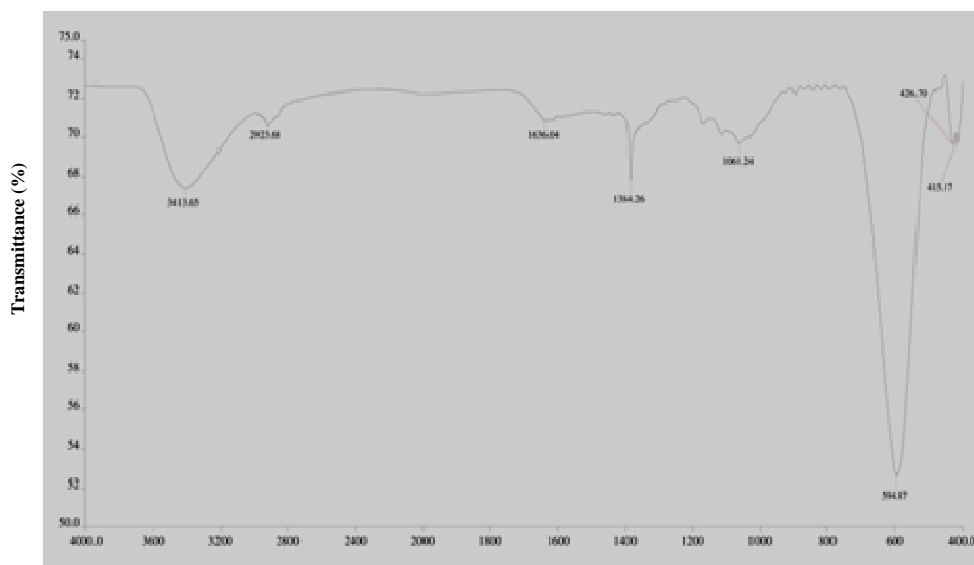
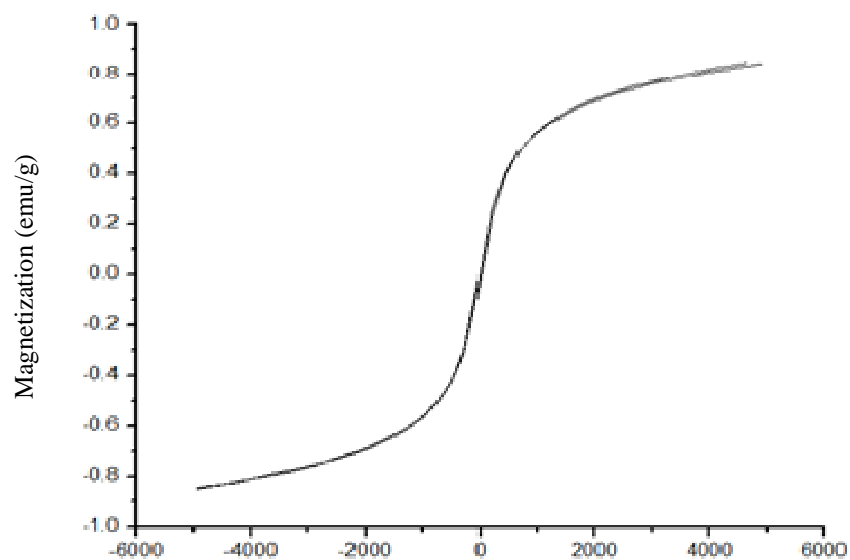
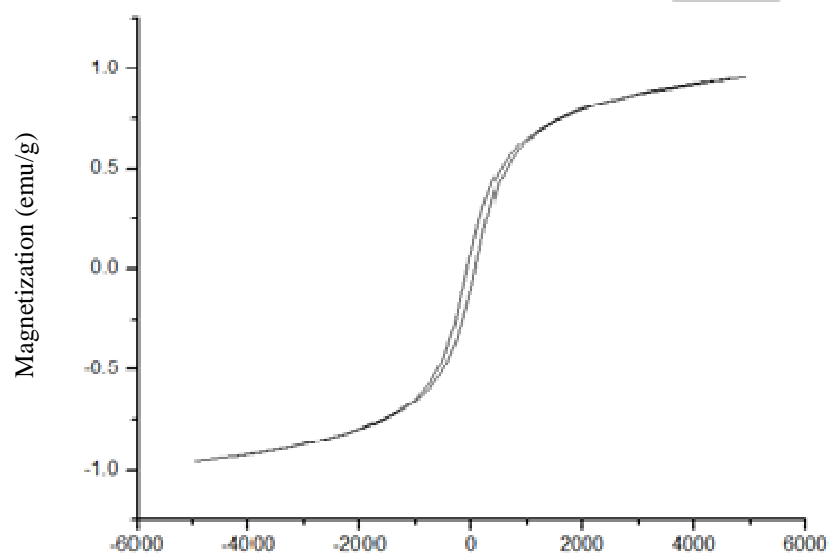
(c) $x = 0.65$ Wave number (cm^{-1})(d) $x = 0.85$ Wave number (cm^{-1})

Figure 3: FTIR spectrographs of nanocrystalline $\text{Ni}_x\text{Zn}_{1-x}\text{Fe}_2\text{O}_4$ ferrites nanoparticles with $x=0.25, 0.45, 0.65, 0.85$ calcined at 600°C for 2h

(a) $x = 0.25$ Applied field (Oe)(b) $x = 0.45$ Applied field (Oe)

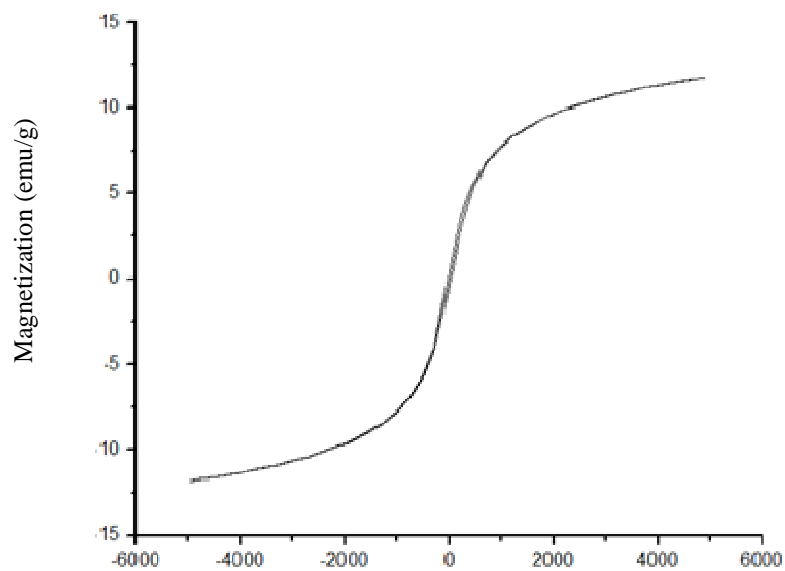
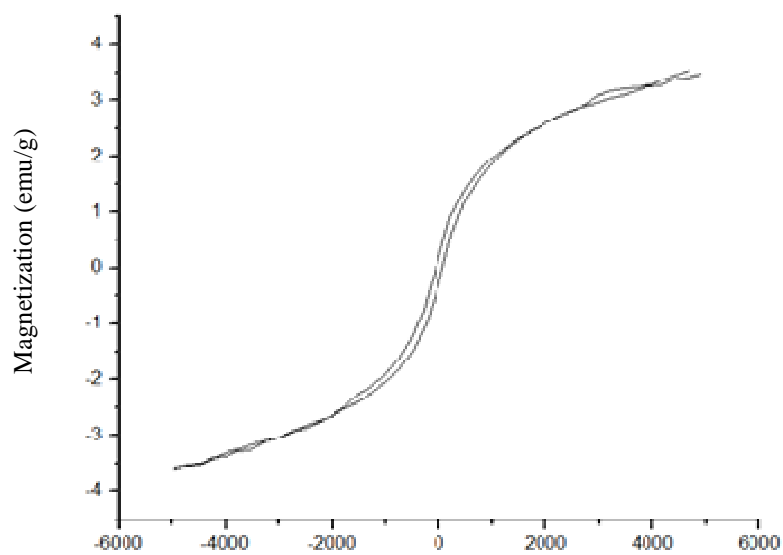
(c) $x = 0.65$ Applied field (Oe)(d) $x = 0.85$ Applied field (Oe)

Figure 4: Hysteresis plots of nanocrystalline $\text{Ni}_x\text{Zn}_{1-x}\text{Fe}_2\text{O}_4$ ferrites with $x=0.25, 0.45, 0.65, 0.85$ calcined at 600°C for 2h

4. CONCLUSIONS

Nanocrystalline $\text{Ni}_x\text{Zn}_{1-x}\text{Fe}_2\text{O}_4$ ferrites with varying x were synthesized by a simple solution route using high purity nitrates and aloe vera plant extract solution. Nanocrystalline $\text{Ni}_x\text{Zn}_{1-x}\text{Fe}_2\text{O}_4$ ferrites with varying x were synthesized. From XRD, FT-IR spectra and TEM analysis, it is indicated that the crystalline spinel ferrite can be obtained using calcination temperature at 600 °C for 2h. XRD pattern confirms the synthesis of fully crystalline single phase Ni-Zn nano ferrites. The particle size of nanocrystalline spinel ferrite calculated from full width at half maximum FWHM of XRD (311) peak are in range of 9 nm-20 nm and in good agreement with TEM result. TEM micrograph studies shows nanocrystalline nature of the samples with average crystallite size between 9nm to 20nm. The room temperature M-H hysteresis curve show paramagnetic behaviour in Ni content up to $\text{Ni} = 0.25$ and show ferromagnetic behaviour in Ni content at $\text{Ni} = 0.45, 0.65, 0.85$. The values of saturation magnetization increases with increase in Ni content up to $\text{Ni} = 0.65$ and then decreases. This work demonstrates the use of a simple synthetic method using cheap precursors of Aloe vera plant extract provides high – yield nanosized ferrites with well crystalline structure and uniform particle sizes, energy saving, high purity, no reaction with containers which increases purity, no pH adjustment, environmental friendly, and acceptable magnetic properties.

ACKNOWLEDGEMENT

Author is grateful to UGC for providing the financial support for carrying

out research work. Author is grateful to SAIF P.U. Chandigarh for characterization like TEM and FTIR of samples. The author is thankful to Physics Dept, NIT Kurukshetra for providing the facilities of XRD. The author is thankful to Physics Dept, M.D. University, Rohtak for providing lab facilities. Author is thankful to Prof R. K. Kotnala from National Physical Laboratory, New Delhi and Prof M. Singh from H. P. University, Shimla for VSM Studies.

REFERENCES

1. Titulaer M K, Jansen J B H and Geus J W. *Clays Clay Miner.* 42,249 (1994).
2. Cao M S, Liu H T, Chen Y J, Wang B and Zhu J. *Sci. Chin.* E 46, 104 (2003).
3. Cao M S, Wang R G, Fang X Y, Cui Z X, Chang T J and Yang H J. *Powder Technol.* 115,1293 (2001).
4. Wang J M, Wang Y F, Jiang C B and Xu H B. *Chin. Phys. Lett.* 23,1293 (2006).
5. Mohapatara M, Brajesh P, Chandan V, Anand S, Das R P and Verma H C. *J. Magan. Mater* 249, 46 (2005).
6. Sugimoto M. *J. Am. Ceram. Soc.* 82 269 (1999).
7. Vucclie M, Jones W and Moggridge G D. *Clays Clay Miner.* 45 803 (1997).
8. Wu Z, Wang X and Wang F. *Chin. Phys. Lett.* 24, 3249 (2007).
9. Busetto C, Del Piero G, Mamara G, Friiro F and Vaccar A. *J. Catal.* 85, 260 (1984).
10. Zhou X D, Qi X and Li F. *Mater. Mech. Engin.* 33, 88 (in Chinese) (2009).
11. Castro S and Gayoso M. *J. Solid State Chem.* 134, 227 (1997).
12. Mydeen K, Yu Y and Jin C. *Chin. Phys. Lett.* 25, 3177 (2008).

- 13 Constantion V R L and Pinnavaia T J. *Inorg. Chem.* 34, 2086 (1998).
- 14 Taylor R M. *Clay Miner.* 15, 369 (1980).
- 15 Sepelak V, Baabe D, Litterst F J and K D Backer. *J. Appl. Phys.* 88, 5884 (2000).
- 16 C. H. Lin, S. Q. Chen, *Chin. J. Mater. Sci.* 15, 31 (1983).
- 17 Z. Yue, Ji Zhou, L. Li, H. Zhang and Z. Gui, *J. Magan. Mater.* 208, 55 (2000).
- 18 Defination, Testing and Application of Aloe Vera and Aloe Vera Gel, *Nature* (2007)
- 19 S.P. Chandran, M. Chaudhary, R Pasricha, A. Ahmad, M. Sastry, *Biotechnol. Prog.* 22, 577 (2006).
- 20 B. D. Cullity, Elements of X-ray Diffraction, Adison-Wesley Publ. Co., London (1967).
- 21 V. R. K. Murthy and J. Sobhanadri, *Phys. Stat. Solidi. A* 36, 133 (1971).
- 22 R. K. Selvan, C.O. Augustin, L.B. Berchmans, R. Sarawathi, *Mater. Res. Bull.* 38, 41 (2003)
- 23 R. D. Waldron, *Phys. Rev.* 99, 1727 (1955).
- 24 S. Yan, J. Geng, L. Yin, E. Zhou, *J. Magn. Mater.* 277, 84 (2001).
- 25 B. D. Cullity, Introduction to Magnetic Materials, Addison-Wesely Publishing Co. Inc., Reading. MA. (1972).
- 26 S. Chikazumi, Physics of Magnetism, Wiley, New York, (1959).
- 27 A. Verma, D.C. Dube, *J. Am. Ceram. Soc.*, 88, 519 (2005).